



EUROPEAN  
HEMATOLOGY  
ASSOCIATION



Ferrata Storti  
Foundation

# HIF1A is a critical downstream mediator for hemophagocytic lymphohistiocytosis

Rui Huang<sup>1,2</sup> Yoshihiro Hayashi,<sup>1,3</sup> Xiaomei Yan,<sup>1</sup> Jiachen Bu,<sup>1,4</sup> Jieyu Wang,<sup>1</sup> Yue Zhang,<sup>1,5</sup> Yile Zhou,<sup>1</sup> Yuting Tang,<sup>1,6</sup> Lingyun Wu,<sup>1</sup> Zefeng Xu,<sup>5</sup> Xin Liu,<sup>4,7</sup> Qianfei Wang,<sup>4,7</sup> Jianfeng Zhou,<sup>6</sup> Zhijian Xiao,<sup>5</sup> James P. Bridges,<sup>8</sup> Rebecca A. Marsh,<sup>9</sup> Kejian Zhang,<sup>10</sup> Michael B. Jordan,<sup>9</sup> Yuhua Li<sup>2</sup> and Gang Huang<sup>1</sup>

RH and YH contributed equally to this work and GH and YHL contributed equally to this study as joint senior authors

<sup>1</sup>Division of Experimental Hematology and Cancer Biology, Cincinnati Children's Hospital Medical Center, OH, USA; <sup>2</sup>Department of Hematology, Zhujiang Hospital, Southern Medical University, Guangzhou, China; <sup>3</sup>Laboratory of Oncology, School of Life Sciences, Tokyo University of Pharmacy and Life Sciences, Japan; <sup>4</sup>Key Laboratory of Genomic and Precision Medicine, Beijing Institute of Genomics, Chinese Academy of Sciences, China; <sup>5</sup>State Key Laboratory of Experimental Hematology, Institute of Hematology and Blood Diseases Hospital, Chinese Academy of Medical Sciences & Peking Union Medical College, Tianjin, China; <sup>6</sup>Department of Hematology, Tongji Hospital, Tongji Medical College, Huazhong University of Science and Technology, Wuhan, Hubei, China; <sup>7</sup>University of Chinese Academy of Sciences, Beijing, China; <sup>8</sup>Perinatal Institute, Division of Pulmonary Biology, Cincinnati Children's Hospital Medical Center, OH, USA; <sup>9</sup>Division of Bone Marrow Transplantation and Immune Deficiency, Cincinnati Children's Hospital, OH, USA and <sup>10</sup>Division of Human Genetics, Cincinnati Children's Hospital Medical Center, OH, USA

Haematologica 2017  
Volume 102(11):1956-1968

## Correspondence:

gang.huang@cchmc.org

Received: June 20, 2017.

Accepted: August 24, 2017.

Pre-published: August 31, 2017.

doi:10.3324/haematol.2017.174979

Check the online version for the most updated information on this article, online supplements, and information on authorship & disclosures: [www.haematologica.org/content/102/11/1956](http://www.haematologica.org/content/102/11/1956)

©2017 Ferrata Storti Foundation

Material published in *Haematologica* is covered by copyright. All rights are reserved to the Ferrata Storti Foundation. Use of published material is allowed under the following terms and conditions:

<https://creativecommons.org/licenses/by-nc/4.0/legalcode>.

Copies of published material are allowed for personal or internal use. Sharing published material for non-commercial purposes is subject to the following conditions:

<https://creativecommons.org/licenses/by-nc/4.0/legalcode>,

sect. 3. Reproducing and sharing published material for commercial purposes is not allowed without permission in writing from the publisher.



## ABSTRACT

Hemophagocytic lymphohistiocytosis (HLH) is a life-threatening syndrome characterized by overwhelming immune activation. A steroid and chemotherapy-based regimen remains as the first-line of therapy but it has substantial morbidity. Thus, novel, less toxic therapy for HLH is urgently needed. Although differences exist between familial HLH (FHL) and secondary HLH (sHLH), they have many common features. Using bioinformatic analysis with FHL and systemic juvenile idiopathic arthritis, which is associated with sHLH, we identified a common hypoxia-inducible factor 1A (HIF1A) signature. Furthermore, HIF1A protein levels were found to be elevated in the lymphocytic choriomeningitis virus infected *Prf1*<sup>-/-</sup> mouse FHL model and the CpG oligodeoxynucleotide-treated mouse sHLH model. To determine the role of HIF1A in HLH, a transgenic mouse with an inducible expression of HIF1A /ARNT proteins in hematopoietic cells was generated, which caused lethal HLH-like phenotypes: severe anemia, thrombocytopenia, splenomegaly, and multi-organ failure upon HIF1A induction. Mechanistically, these mice show type 1 polarized macrophages and dysregulated natural killer cells. The HLH-like phenotypes in this mouse model are independent of both adaptive immunity and interferon- $\gamma$ , suggesting that HIF1A is downstream of immune activation in HLH. In conclusion, our data reveal that HIF1A signaling is a critical mediator for HLH and could be a novel therapeutic target for this syndrome.

## Introduction

Hemophagocytic lymphohistiocytosis (HLH) is a syndrome of overwhelming immune activation characterized by several clinical features, such as high fever, multi-lineage cytopenia, splenomegaly, and hyperferritinemia.<sup>1-3</sup> In primary HLH patients, various mutations in genes related to the granule-dependent cytotoxicity pathway in T/natural killer (NK) cells have been identified.<sup>4</sup> CD8<sup>+</sup> T cells and interferon gamma (IFN- $\gamma$ ) have been shown to play critical roles in the pathogenesis of primary HLH, the onset of which is usually triggered by viral infection.<sup>5</sup> On the other hand, secondary HLH (sHLH) has a heterogeneous etiology, which is often

triggered by systemic viral infection, autoimmune disorder, or hematologic malignancies.<sup>3,6</sup> In contrast to primary HLH, cytotoxic activity of T/NK cells is not always decreased in sHLH.<sup>7</sup> Macrophage activation syndrome (MAS), a form of sHLH in the context of rheumatic disease that is especially associated with systemic juvenile idiopathic arthritis (sJIA),<sup>8</sup> is associated with aberrant toll-like receptor (TLR)-induced gene expression patterns.<sup>9</sup> Despite reports that primary and sHLH have different genetic aberrations and distinct cytotoxic activities, the key features for HLH (cytopenias and a unique presentation of extreme inflammation) remain common.<sup>7</sup> Thus, we hypothesized that there are common underlying downstream mediators for HLH phenotype development. Identifying these mediators for HLH will not only help to understand the disease, but also lead to the development of better therapies.

Hypoxia-inducible factor (HIF), which was originally discovered as a critical transcription factor for optimal cellular adaptation to hypoxia, actually plays an important role in immune response, both in hypoxia and normoxia conditions<sup>10,11</sup> HIF consists of heterodimers, HIF- $\alpha$  subunit and ARNT. ARNT is stably expressed in many cell types, while HIF- $\alpha$  subunits are expressed differently in tissues and cells. So far, three isoforms of HIF- $\alpha$  subunits, HIF1A, HIF2A, and HIF3A, have been documented.<sup>12</sup> HIF1A is widely expressed in both innate and adaptive immune cells,<sup>15-16</sup> while HIF2A/EPAS1 expression is limited in certain immune cell types,<sup>17,18</sup> and the HIF3A expression pattern has not been so well studied. Many stimuli or factors that have a function in the immune response lead to HIF1A protein accumulation and activation independent of the hypoxic regulation. Bacteria, lipopolysaccharide (LPS), and tumor necrosis factor- $\alpha$  (TNF- $\alpha$ ) have been well documented to induce HIF1A accumulation in macrophages, thereby boosting their microbicidal capacity.<sup>19,20</sup> T-cell receptor ligation in T cells increases HIF1A transcription and HIF1A protein accumulation. Moreover, cytokines, such as IL-2, induce HIF1A accumulation in CD8<sup>+</sup> T cells enhancing their cytotoxic function.<sup>10</sup> There is growing evidence to indicate the potential role of HIF1A signaling in immune activation.

To identify the key downstream mediators for HLH, we first performed a bioinformatic analysis of published microarray expression datasets of familial hemophagocytic lymphohistiocytosis (FHL) and sJIA.<sup>9,21</sup> We found that the HIF1A signature, which refers to a group of HIF1A-induced genes, was enriched in both FHL and sJIA patients' peripheral blood mononuclear cells (PBMCs). Then, we confirmed that HIF1A protein expression was significantly increased in two widely-used HLH mouse models. Furthermore, *in vivo* data from transgenic mice show that activation of HIF1A in hematopoietic cells results in HLH-like phenotypes. Our study suggests that the HIF1A signaling pathway is a critical pathological downstream mediator for HLH development.

## Methods

### Cell line and mice

Murine cell line Raw264.7 was purchased from ATCC. Cells were cultured in DMEM medium in a 5% CO<sub>2</sub> incubator at 37°C, and subcultured every 2-3 days. *Rag1*<sup>-/-</sup>, *Ifng*<sup>-/-</sup>, *Ifng*<sup>-/-</sup>, *Prf1*<sup>-/-</sup>, *Vav1*-

*Cre*, and *Rosa26-LSL-rtTA* mice were purchased from Jackson Laboratory. Transgenic HIF1A-TPM mice were kindly provided by Professor James Bridge from Cincinnati Children's Hospital Medical Center (CCHMC).<sup>22</sup> Mice, with the genotype of *Ncr1-iCre*, were kindly provided by Professor Eric Vivier from the French INSERM Laboratory.<sup>23</sup> LCMV-infected *Prf1*<sup>-/-</sup> mouse model and the repeated CpG-treated mouse model were generated as previously described.<sup>5,24,25</sup> All animal studies were performed according to an approved Institutional Animal Care and Use Committee protocol and federal regulations.

### Statistical analysis

Data were analyzed by Prism 6.0 (GraphPad Software). *P* < 0.05 was considered significant. Continuous variables were analyzed by using Student *t*-test or one-way ANOVA. Mice survival was estimated using the Kaplan-Meier method.

Information concerning the antibodies and reagents, bioinformatic analysis, flow cytometry, ELISA, western blot, histology, generation of bone marrow-derived macrophages, and the assay used to determine the capacity of macrophages to engulf erythroblasts is reported in detail in the *Online Supplementary Appendix*.

## Results

### Activated HIF1A signaling in FHL and sJIA patients

Immune activation is coupled with cytokine signaling and transcriptional changes. To investigate the network of transcription factors in HLH pathogenesis, we took a bioinformatic approach and analyzed two published microarray datasets of patients with FHL and sJIA.<sup>9,21</sup> Since there are no available sHLH transcript profile data, we utilized the microarray data of sJIA patients which are more likely to be complicated by macrophage activation syndrome, a subtype of sHLH in the context of rheumatoid diseases.<sup>26-28</sup> We performed unbiased TF-target enrichment analysis<sup>29</sup> and found that HIF1A, NF- $\kappa$ B, GATA1, and STAT1 are the common immune-related transcription factors in both the FHL and sJIA datasets (Figure 1A and B and *Online Supplementary Figure S1A and B*). Among these transcription factors, HIF1A is of particular interest as it regulates not only the up-regulated genes but also the down-regulated genes in HLH, indicating that HIF1A might be a critical mediator in HLH development. HIF1A is known to be regulated in both transcriptional and post-translational levels. In the FHL dataset, *HIF1A* mRNA is increased in the FHL patients compared to healthy donors; however, there is no significant difference in HIF1A expression between FHL patients with and those without a genetic diagnosis (*Online Supplementary Figure S1C and D*). At the same time, in the sJIA dataset, there is no significant change in HIF1A expression at the mRNA level between patients and healthy donors (*Online Supplementary Figure S1E*).

To investigate enrichment of the HIF1A signature in HLH, we also utilized another bioinformatic approach of gene set enrichment analysis (GSEA) to analyze these two datasets, and revealed that the HIF1A signature is significantly enriched in both the FHL and sJIA PBMCs datasets (Figure 1C and D). However, there is no significant difference in HIF1A signature enrichment between FHL patients with and those without a genetic diagnosis (*Online Supplementary Figure S1F*). There are 258 leading edge genes (LEGs) in the FHL dataset and 214 LEGs in the sJIA

dataset with 108 overlapping common LEGs (Figure 1E). Gene ontology analysis showed that these overlapping common LEGs are related to blood coagulation, chemotaxis, glycolysis, oxygen species metabolic process, platelet activation, immune response, and cytokines (Figure 1E). These results further suggest that HIF1A may play a key role in regulating downstream targets in both primary HLH and sHLH patients.

**Elevated HIF1A protein in LCMV-infected *Prf1*<sup>-/-</sup> and CpG-treated mouse HLH models**

Several mouse models that recapitulate primary HLH, sHLH, or MAS have been reported.<sup>7</sup> We determined whether HIF1A signaling is activated in established HLH mouse models. The LCMV-infected perforin-deficient (*Prf1*<sup>-/-</sup>) mouse model is a well-known HLH mouse model that recapitulates biallelic perforin mutation patients with

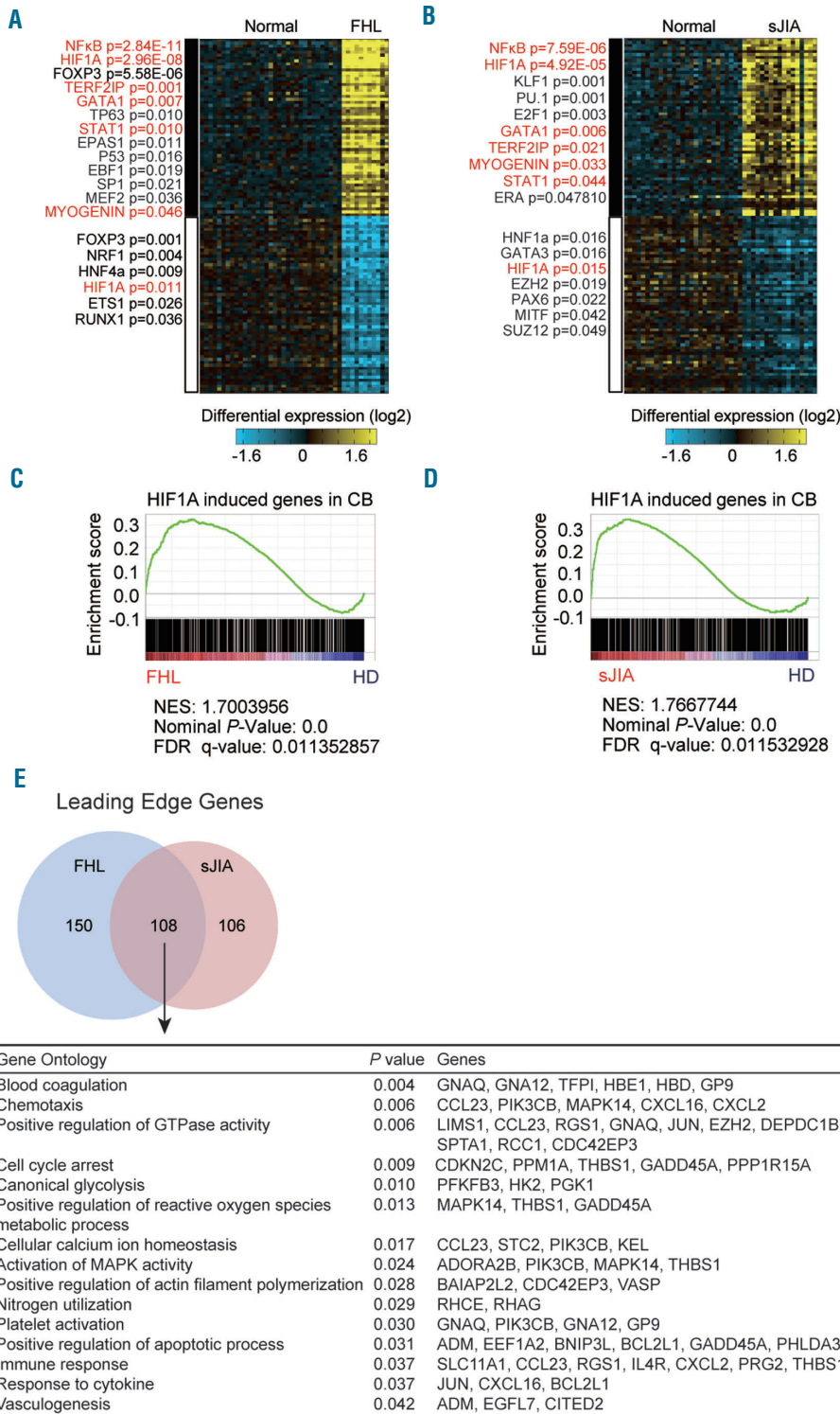


**Figure 1. HIF1A signature is enriched in familial hemophagocytic lymphohistiocytosis (FHL) and systemic juvenile idiopathic arthritis (sJIA) patients.** (A and B) Heatmaps showing differentially expressed genes with more than a 1.5-fold difference in expression comparing peripheral blood mononuclear cells (PBMCs) from FHL patients (n=11) with healthy donors (n=33) based on a published microarray dataset (GSE26050) (A) and from sJIA patients (n=17) with healthy donors (n=30) based on a published microarray dataset (GSE7753). (B) To the left of the heatmap are top predicted transcription factors using transcription factor-target enrichment analysis using the Go-Elite algorithm in AltAnalyze software. The common predicted transcription factors in both FHL and sJIA datasets are marked in red. (C and D) Gene set enrichment analysis (GSEA) plot showing an increase in gene expression of HIF1A-induced genes in FHL microarray dataset (C) and sJIA dataset (D). Up-regulated genes (fold change >2.0) in HIF1A over-expressed human cord blood (CB) CD34<sup>+</sup> cells serve as the HIF1A-induced genes (Genomic Spatial Event database; GSE 54663). Normalized enrichment score (NES), P-value, and false discovery rate (FDR) are shown. (E) Venn diagram showing the overlap of the leading edge genes from GSEA comparing FHL and sJIA datasets. Tabular data showing gene ontology (GO) analysis to the overlapping leading edge genes.

pathogen infection (Figure 2A).<sup>5</sup> After challenging them with LCMV, the *Prf1*<sup>-/-</sup> mice quickly developed anemia and thrombocytopenia (Figure 2B). CD8<sup>+</sup> T cells activate macrophages *via* secreting IFN- $\gamma$  in this mouse model. We measured HIF1A expression levels in Gr1<sup>+</sup>CD115<sup>+</sup>F4/80<sup>+</sup>SSC<sup>low</sup> spleen macrophages by using flow cytometry (Figure 2C)<sup>30</sup> and found that HIF1A levels in spleen macrophages were significantly increased in LCMV-infected *Prf1*<sup>-/-</sup> mice compared to the control mice (Figure 2D). We also identified profound type 1 polarized macrophages in the spleen (Figure 2E and F) and bone marrow (*data not shown*) from the LCMV-infected *Prf1*<sup>-/-</sup> mice.

Repeated injections of TLR9 ligand CpG oligodeoxynucleotides (ODN) causes sHLH in wild-type (WT) mice,<sup>24</sup> which mimics sHLH features (Figure 2G). After injecting CpG five times into WT mice, CpG-treated-mice developed anemia and thrombocytopenia (Figure 2H). Similar to what was observed in the primary HLH model, we found that HIF1A expression in the spleen macrophages was also increased in CpG-treated mice (Figure 2I). Type 1 polarization of macrophages in spleen (Figure 2J and K) and bone marrow (*data not shown*) was observed in CpG-treated mice. Taken together, these data suggest that HIF1A protein expression is elevated both in primary HLH and sHLH mouse models.

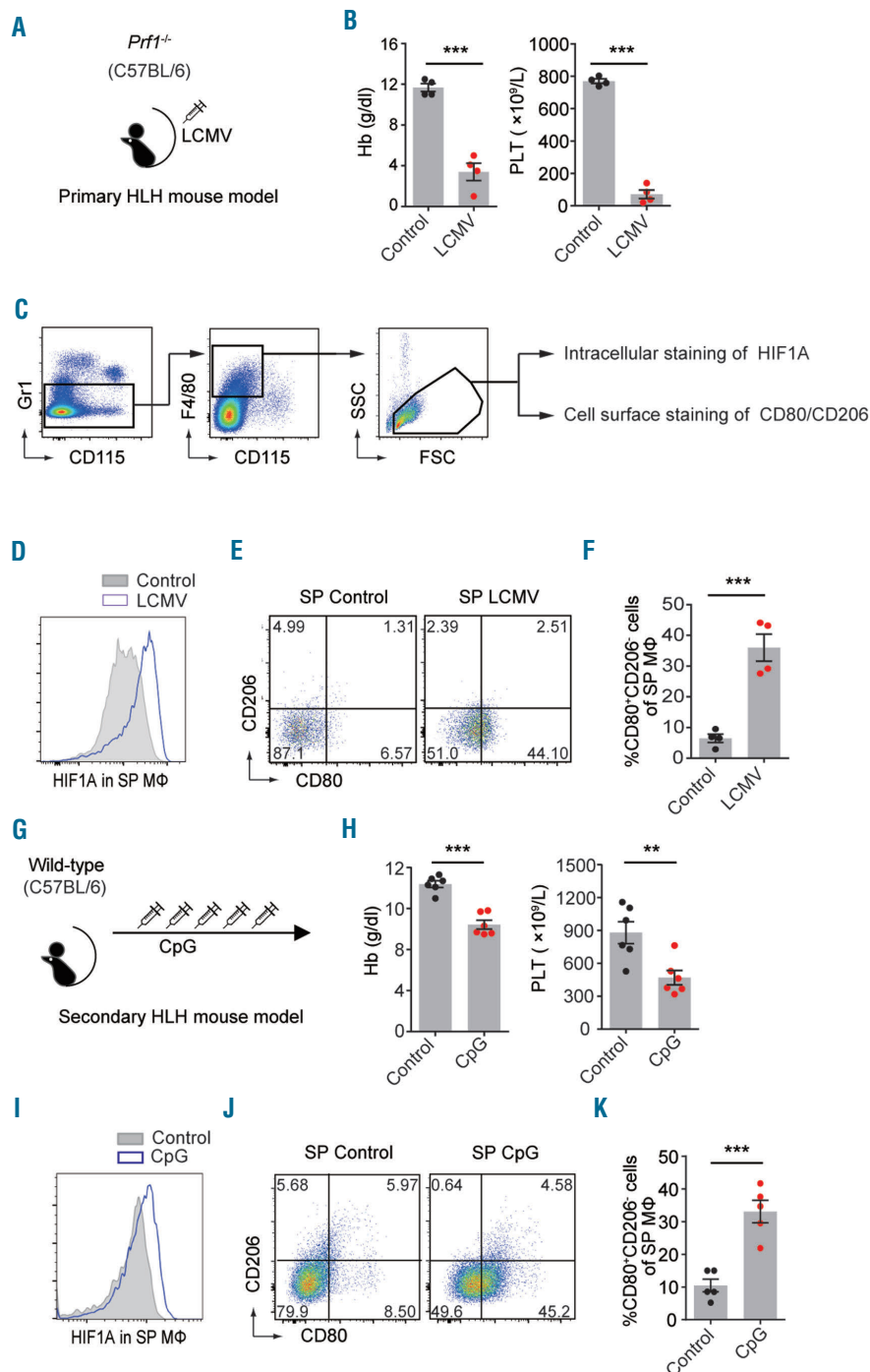


**Figure 2. HIF1A protein in macrophages is elevated in hemophagocytic lymphohistiocytosis (HLH) mouse models.** (A) Schematic diagram depicting lymphocytic choriomeningitis virus (LCMV)-infected *Prf1*<sup>-/-</sup> HLH mouse model. Perforin-deficient (*Prf1*<sup>-/-</sup>) mice were infected with or without LCMV-WE of 200 plaque-forming units (PFU) via intraperitoneal injection. Mice were sacrificed and analyzed on day (d)14 after inoculation. (B) Hemoglobin (Hb) and platelets (PLT) of LCMV-infected or non-infected *Prf1*<sup>-/-</sup> mice. (C) Flow cytometry gating strategy showing splenic macrophages identified as Gr1<sup>+</sup>CD115<sup>+</sup>SSC<sup>low</sup>F4/80<sup>+</sup> from indicated mice. (D) Flow cytometry histogram plot showing HIF1A level in splenic macrophages in indicated mice. The tinted gray histogram represents an LCMV-infected *Prf1*<sup>-/-</sup> mouse. The blue histogram represents a non-infected *Prf1*<sup>-/-</sup> mouse. Plot is representative of 4 independent intracellular stainings. (E) Flow cytometry dot plot showing CD80 and CD206 expression in splenic macrophages in LCMV-infected or non-infected mice. Plots are representative of 4 independent stainings. (F) Quantitative analysis of percentage of CD80<sup>+</sup>CD206<sup>+</sup> macrophages in total splenic macrophages in indicated mice. (G) Schematic diagram showing repeated CpG-treated HLH mouse model. CpG (75  $\mu$ g) or PBS was injected i.p. to wild-type mice on days 0, 2, 4, 6, 8. On d9, mice were sacrificed and analyzed. (H) Hb and PLT of CpG or PBS treated mice on d9. (I) Flow cytometry histogram plot showing HIF1A level of splenic macrophages in indicated mice. The tinted gray histogram represents a CpG-treated mouse. The blue histogram represents a PBS-treated mouse. Plot is representative of 3 independent experiments. (J) Flow cytometry dot plots showing CD80 and CD206 expression in splenic macrophages in CpG or PBS-treated mice. Plots are representative of 3 independent experiments. (K) Quantitative analysis of percentage of CD80<sup>+</sup>CD206<sup>+</sup> macrophages in total splenic macrophages in CpG or PBS-treated mice. Plots are representative of 3 independent experiments. \*\**P*<0.01, \*\*\**P*<0.001 versus control. Individual symbols each represent one mouse. PFU: plaque-forming units.

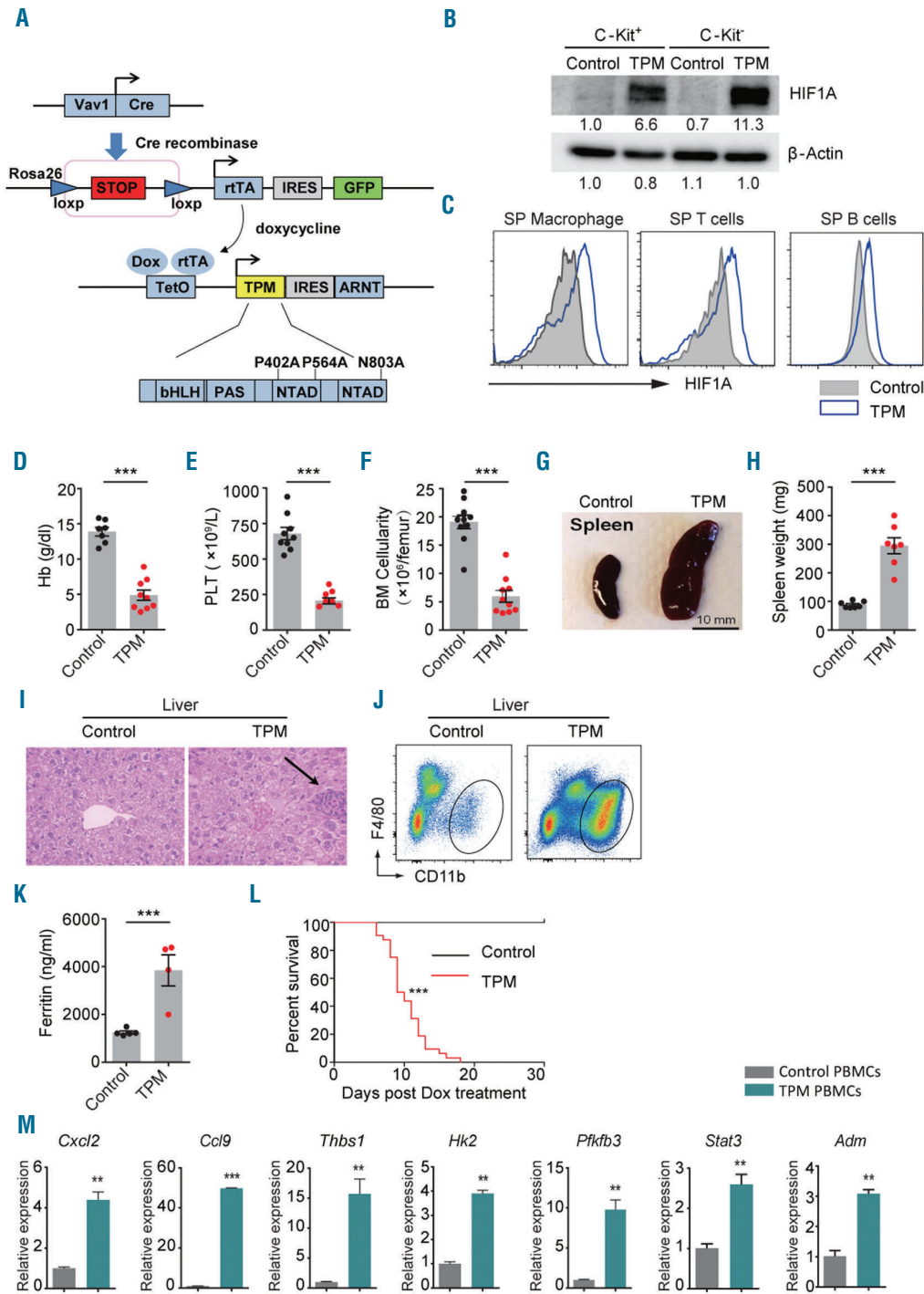


**Figure 3. Induction of HIF1A/ARNT allele in hematopoietic cells in C57BL/6 mice develops features of hemophagocytic lymphohistiocytosis (HLH).** (A) Schematic diagram of inducible HIF1A/ARNT transgenic mouse and HIF1A triple point mutant (TPM) under the *Vav1-Cre* driver. (B) HIF1A protein expression in *c-Kit*<sup>+</sup> and *c-Kit*<sup>-</sup> cells from bone marrow of *Vav1-Cre/TPM* mice and control mice shown by western blot. (C) Flow cytometry histogram plot showing HIF1A level in splenic macrophages gated on Gr1<sup>+</sup>CD115<sup>+</sup>F4/80<sup>+</sup> cells, T cells gated on CD3<sup>+</sup> cells, B cells gated on B220<sup>+</sup> cells. The tinted gray histogram represents a *Vav1-Cre*/wild-type (WT) mouse, the blue histogram represents a *Vav1-Cre/TPM* mouse. (D-I) *Vav1-Cre/TPM* mice and control mice were administered with doxycycline, sacrificed and analyzed on day (d)8. Hemoglobin (Hb) (D), platelet (PLT) (E), and bone marrow (BM) cellularity of one femur (F) were shown. (G-I) Representative plot of spleen (SP) (G), quantitative analysis of spleen weight (H) and representative plot of liver (I) were shown. (J and K) Liver sections of *Vav1-Cre/TPM* mice and control mice on d4 were stained by H&E. (J) Representative plots at an original magnification of  $\times 400$ . Infiltrates are marked with black arrow. (K) Representative scattered dot plots indicating infiltration of CD11b<sup>+</sup> myeloid cells (gated on CD45<sup>+</sup> cells) into liver. (L) Serum ferritin levels of *Vav1-Cre/TPM* mice and control mice were measured by ELISA at end point of survival. (M) Kaplan-Meier analysis of survival of *Vav1-Cre/TPM* mice (n=32) and control mice (n=26). (N) Relative mRNA expression of selected genes from the common leading edge genes of GSEA of FHL and sJIA datasets was measured in PBMCs from *Vav1-Cre/TPM* mice (n=3) and control mice (n=3) by qRT-PCR. Data are representative of 3 independent experiments. Depicted data are from at least 3 independent experiments. Individual symbol in dot plots each represents one mouse. \*\**P*<0.01, \*\*\**P*<0.001 versus control for all experiments. GSEA: gene set enrichment analysis; sJIA: systemic juvenile idiopathic arthritis.

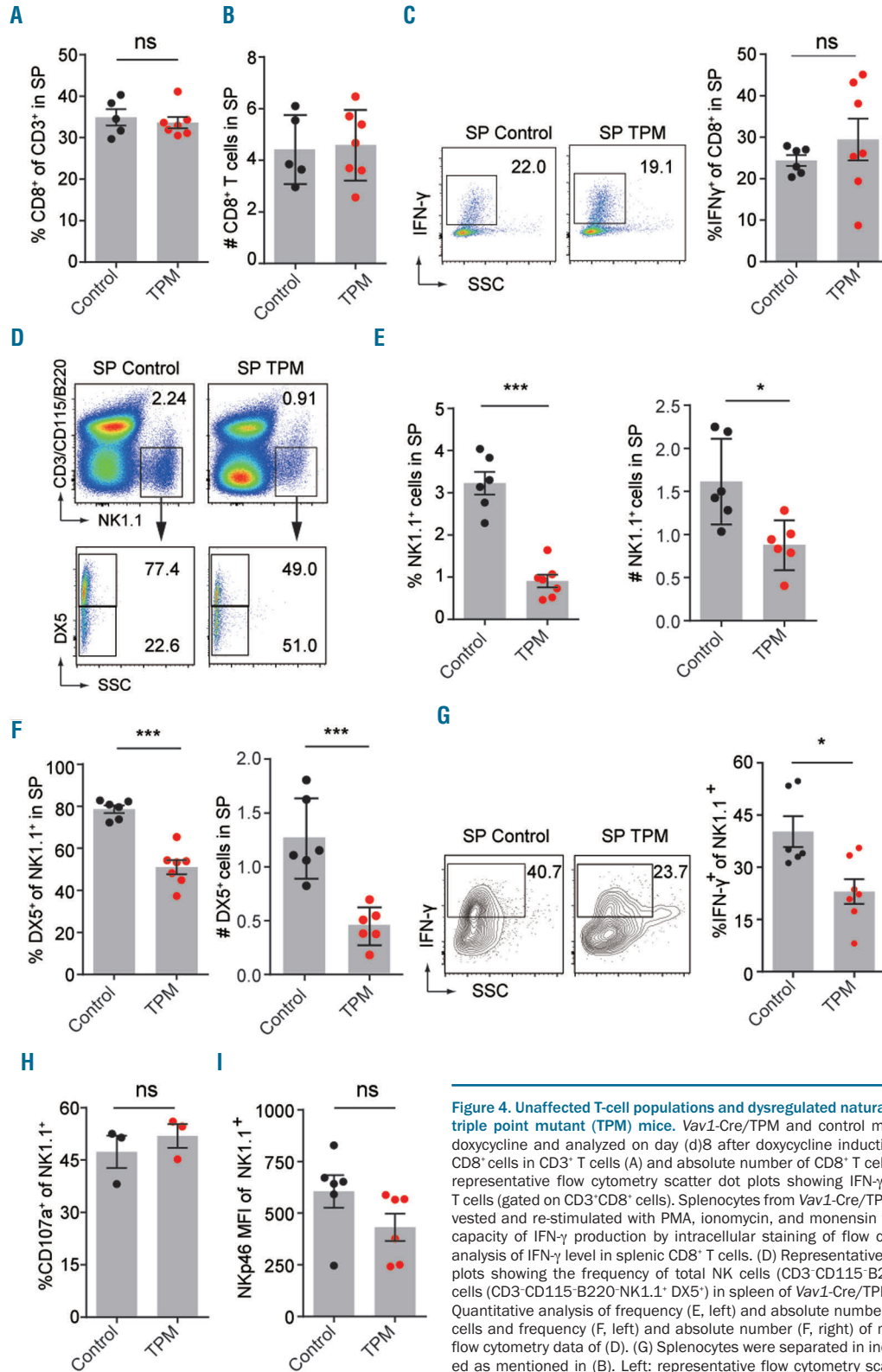


**Figure 4. Unaffected T-cell populations and dysregulated natural killer (NK) cells in inducible triple point mutant (TPM) mice.** *Vav1-Cre/TPM* and control mice were administrated with doxycycline and analyzed on day (d)8 after doxycycline induction. (A and B) Percentage of CD8<sup>+</sup> cells in CD3<sup>+</sup> T cells (A) and absolute number of CD8<sup>+</sup> T cells (B) in spleen (SP). (C) Left: representative flow cytometry scatter dot plots showing IFN- $\gamma$  production in splenic CD8<sup>+</sup> T cells (gated on CD3<sup>+</sup>CD8<sup>+</sup> cells). Splenocytes from *Vav1-Cre/TPM* and control mice were harvested and re-stimulated with PMA, ionomycin, and monensin for 5 hours to determine the capacity of IFN- $\gamma$  production by intracellular staining of flow cytometry. Right: quantitative analysis of IFN- $\gamma$  level in splenic CD8<sup>+</sup> T cells. (D) Representative flow cytometry scattered dot plots showing the frequency of total NK cells (CD3<sup>+</sup>CD115<sup>+</sup>B220<sup>+</sup>NK1.1<sup>+</sup>) and mature NK cells (CD3<sup>+</sup>CD115<sup>+</sup>B220<sup>+</sup>NK1.1<sup>+</sup>DX5<sup>+</sup>) in spleen of *Vav1-Cre/TPM* and control mice. (E and F) Quantitative analysis of frequency (E, left) and absolute number (E, right) of total splenic NK cells and frequency (F, left) and absolute number (F, right) of mature splenic NK cells from flow cytometry data of (D). (G) Splenocytes were separated in indicated mice and re-stimulated as mentioned in (B). Left: representative flow cytometry scatter dot plots showing IFN- $\gamma$  production in splenic NK cells (gated on CD3<sup>+</sup>CD115<sup>+</sup>B220<sup>+</sup>NK1.1<sup>+</sup> cells). Right: quantitative analysis of IFN- $\gamma$  production in splenic NK cells from flow cytometry data of (G). (H) Quantitative analysis of CD107a expression of splenic NK cells (gated on CD3<sup>+</sup>CD115<sup>+</sup>B220<sup>+</sup>NK1.1<sup>+</sup> cells). (I) Quantitative analysis of Nkp46 expression of splenic NK cells (gated on CD3<sup>+</sup>CD115<sup>+</sup>B220<sup>+</sup>NK1.1<sup>+</sup> cells). Depicted data are representative of 3 independent experiments. Individual symbol in dot plots each represents one mouse. \**P*<0.05, \*\**P*<0.01, \*\*\**P*<0.001 versus control for all experiments. #: absolute number; ns: not significant.

**Inducible activation of HIF1A is sufficient for developing HLH-like phenotypes in C57BL/6 background mice**

To determine the significance of HIF1A signaling activation in HLH development *in vivo*, we generated transgenic mice with inducible HIF1A/ARNT expression in hematopoietic cells. We combined the Vav1-Cre allele, Rosa26-loxp-stop-loxp (LSL) reverse-tetracycline-controlled transactivator (rtTA) allele, and triple point mutation (TPM) HIF1A /wild-type ARNT alleles (tet-on-TPM/ARNT) (Vav1-Cre/TPM). Triple point mutations

include P402A, P564A and N803A, which prevent degradation and facilitate transcriptional activation of HIF1A.<sup>22</sup> Thus, Vav1-Cre/TPM mice have stabilized and constitutively active HIF1A protein (Figure 3A) in hematopoietic cells after administration of doxycycline. Vav1-Cre mice without the TPM allele (Vav1-Cre/WT) served as control. We confirmed an increase in HIF1A protein level in both c-Kit positive and negative cells (Figure 3B) by western blot and in individual cell lineages by flow cytometry (Figure 3C) in Vav1-Cre/TPM mice compared to control mice. Importantly, the level of HIF1A in macrophages in

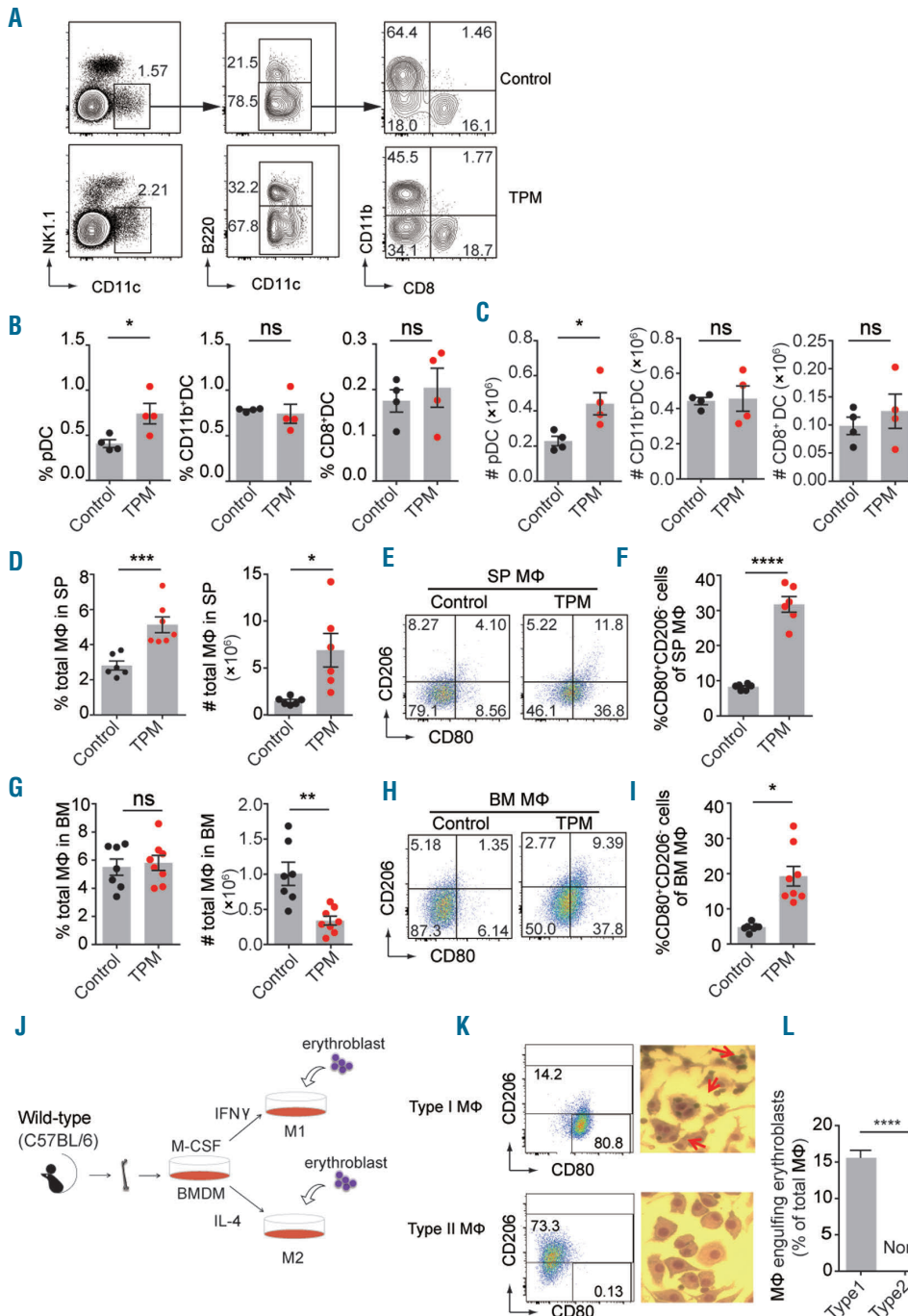


**Figure 5. Dendritic cells (DCs) are slightly changed but macrophages are strongly polarized in triple point mutation (TPM)-induced mice.** Vav1-Cre/TPM and control mice were administrated with doxycycline, DCs and macrophages were analyzed. (A) Representative flow cytometry scatter dot plots showing splenic DCs from Vav1-Cre/TPM and control mice on day (d)4 after doxycycline induction. Plasmacytoid DCs (pDCs) are identified as NK1.1<sup>+</sup>CD11c<sup>+</sup>B220<sup>+</sup>CD11b<sup>-</sup>CD8<sup>-</sup> cells. CD11b<sup>+</sup> conventional DCs (cDCs) are identified as NK1.1<sup>-</sup>CD11c<sup>-</sup>B220<sup>-</sup>CD11b<sup>+</sup>CD8<sup>+</sup> cells. CD8<sup>+</sup> cDCs are identified as NK1.1<sup>-</sup>CD11c<sup>-</sup>B220<sup>-</sup>CD11b<sup>+</sup>CD8<sup>+</sup> cells. (B and C) Quantitative analysis of frequency (B) and absolute number (C) of pDCs, CD11b<sup>+</sup> cDCs, and CD8<sup>+</sup> cDCs in spleen cells on d4. (D-I) Quantitative analysis of frequency and absolute number of total macrophage in spleen (SP) (D) and bone marrow (BM) (G). Representative flow cytometry CD80/CD206 scatter dot plots of splenic macrophages (E) and BM macrophages (H). Quantitative analysis of percentage of CD80<sup>+</sup>CD206<sup>-</sup> macrophages in spleen (F) and BM (I). (J) Schematic diagram depicting assay measuring the ability of polarized macrophages to engulf erythroblast. BMDM from wild-type mice were incubated with IFN-γ for 48 hours (h) to polarize towards type 1, or with IL-4 for 24 h to polarize towards type 2, followed by co-culturing with erythroblasts for 12 h. (K) Representative flow cytometry CD80/CD206 scatter dot plots (left) of cultured BMDM. Cytospin was made followed by Giemsa staining. Engulfment of erythroblasts by polarized BMDM was observed under the microscope (right). (L) Quantitative analysis of percentage of macrophages engulfing erythroblasts of total macrophages. Depicted data are representative of at least 3 independent experiments. Individual symbol in dot plots each represents one mouse. \*P<0.05, \*\*\*P<0.001 versus control for all experiments. #: absolute number; ns: not significant; MΦ: macrophage.

TPM mice is comparable to that in CpG-injected HLH mice (*Online Supplementary Figure S2*).

After doxycycline administration, TPM mice with the pure C57BL/6 background quickly developed severe anemia and thrombocytopenia (Figure 3D and E). Bone marrow cellularity was dramatically reduced in the TPM mice (Figure 3F and *Online Supplementary Figure S3A*). We did not find a blockade of erythropoiesis in the bone marrow and spleen from *Vav1-Cre/TPM* mice (*Online Supplementary Figure S4*), indicating a cell extrinsic mechanism for quick progression of anemia and a decrease in bone marrow cellularity. Consistent with the diagnostic criteria for HLH, TPM mice showed splenomegaly (Figure 3G and H). Normal splenic follicular architecture was disrupted in the TPM mice (*Online Supplementary Figure S3B*). Liver dysfunction is commonly observed in HLH patients. Indeed, TPM mice had substantial inflammatory cells infiltrated into the liver (Figure 3I). Flow cytometric analysis revealed that most of these cells were CD11b<sup>+</sup> myeloid cells (Figure 3J). However, we failed to find robust hemophagocytosis in the cytopsin or sections of bone marrow,

spleen, or liver (*data not shown*). High levels of serum ferritin, which is also one of the diagnostic criteria for HLH, was observed in the TPM mice in comparison with the control mice (Figure 3K). Furthermore, several inflammatory cytokines, such as IL-6, IL-12, and IFN- $\gamma$ , were increased in the serum from the TPM mice (*Online Supplementary Figure S5*). All of the mice succumbed within three weeks (Figure 3L). We further confirmed that several genes related to chemokine, macrophage activation, and glycolysis (which are the common LEGs of HIF1A signature in FHL and sJIA datasets), were elevated in the *Vav1-Cre/TPM* mice (Figure 3M and *Online Supplementary Figure S6*). Taken together, inducible expression of stabilized and active HIF1A with ARNT gives rise to HLH-like phenotypes in pure C57BL/6 background mice.

### Unaffected T-cell populations and dysregulated NK cells in induced TPM mice

Given that robust activation of CD8<sup>+</sup> T cells is observed in the primary HLH mouse model, we first determined the T-cell populations in TPM mice. However, no significant

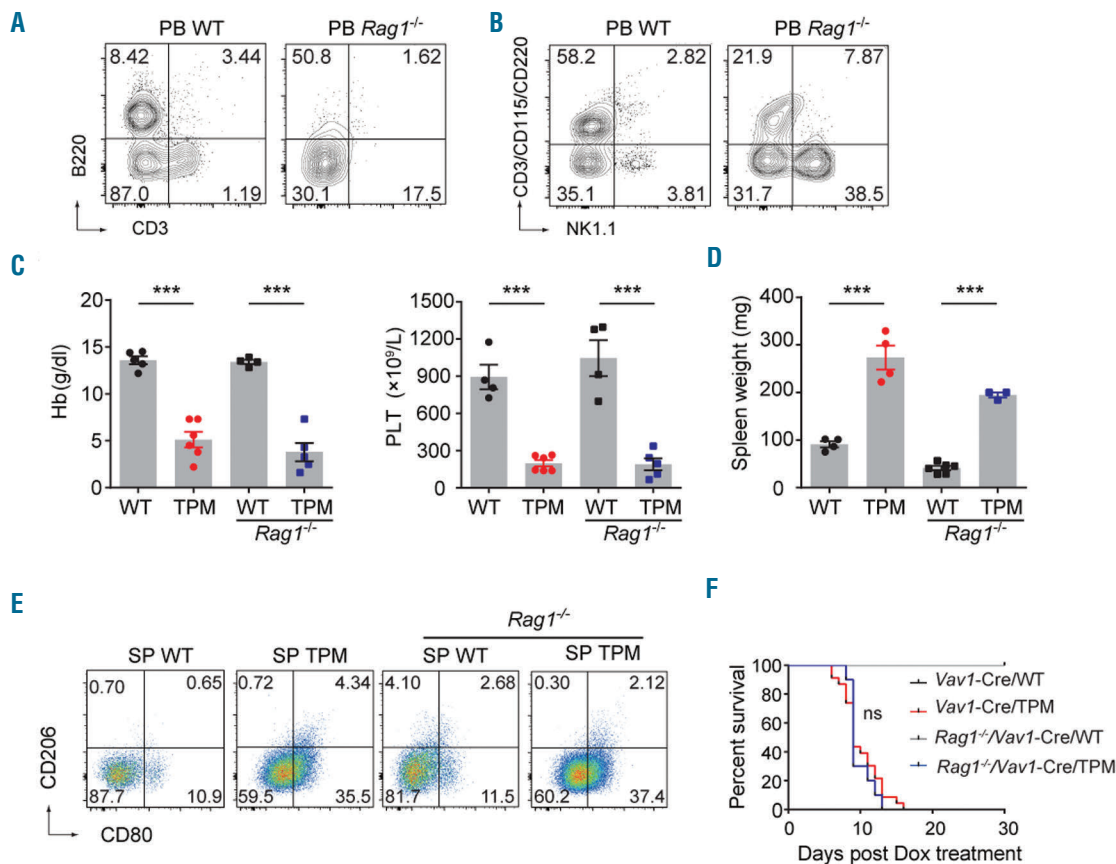


**Figure 6. Adaptive immunity is not required for triple point mutation (TPM)-induced anemia, thrombocytopenia, and macrophage polarization.** *Rag1*<sup>-/-</sup>/*Vav1-Cre/LSL/TPM* (*Rag1*<sup>-/-</sup>/TPM) mice were generated. *Rag1*<sup>-/-</sup>/*Vav1-Cre/LSL/WT* (*Rag1*<sup>-/-</sup>/WT) mice served as their control. *Rag1*<sup>-/-</sup>/TPM, *Rag1*<sup>-/-</sup>/WT, *Vav1-Cre/TPM*, *Vav1-Cre/WT* mice were administrated with doxycycline. (A and B) Representative flow cytometry scatter dot plots showing percentage of T, B cells (A) and natural killer (NK) cells (B) in peripheral blood (PB) in *Rag1*<sup>-/-</sup> and wild-type mice. (C and D) Mice were administrated with doxycycline and analyzed on day (d)8 after doxycycline induction. Hemoglobin (Hb), platelets (PLT) (C) and spleen (SP) weight (D) are shown. (E) Representative flow cytometry CD80/CD206 scatter dot plots of splenic macrophages. (F) Kaplan-Meier analysis of survival of *Rag1*<sup>-/-</sup>/TPM (n=8), *Rag1*<sup>-/-</sup>/WT (n=8), *Vav1-Cre/TPM* (n=32), *Vav1-Cre/WT* (n=26) mice. Statistical analysis showed that there was a significance between *Rag1*<sup>-/-</sup>/TPM and *Rag1*<sup>-/-</sup>/WT mice ( $P < 0.0001$ ), but no significance between *Rag1*<sup>-/-</sup>/TPM and *Vav1-Cre/TPM* mice ( $P > 0.05$ ). Depicted data are representative of 3 independent experiments. Individual symbol in dot plots each represents one mouse. \*\*\* $P < 0.001$  versus control for all experiments. ns: non-significance.

change in the frequency and absolute number of CD8<sup>+</sup> T cells was observed in the TPM mice (Figure 4A and B). We also measured IFN- $\gamma$  production in CD8<sup>+</sup> T cells and did not find a significant difference between the TPM mice and the control mice (Figure 4C), indicating that CD8<sup>+</sup> T cells may not play a key role in HIF1A induced HLH-like phenotypes.

Natural killer cell activity is important for immune homeostasis. NK cell defect is one of the critical features of primary HLH. Reduced NK cell number or impaired NK cell function has been reported in some of the sHLH patients. Interestingly, we found a significant reduction in the number of total NK cells and DX5<sup>+</sup> mature NK cells in the spleen (Figure 4D-F), peripheral blood and bone marrow (*data not shown*) from the TPM mice. Importantly, IFN- $\gamma$  production in NK cells was impaired in the TPM mice (Figure 4G). However, cell surface CD107a expression in NK cells was comparable between the TPM mice and the control mice (Figure 4H), suggesting no major defect in degranulation of cytotoxic granules in TPM mice. It has been reported that hypoxia may lead to a reduction in Nkp46 expression, an NK cell activating receptor, *in vitro*.<sup>31</sup> However, there was no significant difference in Nkp46 expression between the TPM mice and the control mice (Figure 4I). These data suggest that TPM mice have quantitative and functional dysregulation in NK cells.

To determine whether the impairment of NK cells is due to intrinsic or extrinsic NK cell factors, we generated *Ncr1-iCre* /LSL/TPM (*Ncr1-iCre*/TPM) mice. Using GFP reporter, we confirmed that *Ncr1-iCre* is specifically expressed in NK cells (*Online Supplementary Figure S7A and C*).<sup>23</sup> Surprisingly, after NK cell specific TPM induction, we did not find any changes in the NK cell number or differentiation pattern compared to the control mice (*Online Supplementary Figure S7B and D*), indicating that the NK cell dysregulation in *Vav1-Cre*/TPM mice may be due to a non-autonomous cellular mechanism.

#### Slightly changed dendritic cells but strongly polarized Type 1 macrophages in induced TPM mice

Since a minor fraction of dendritic cells (DCs) persistently present antigens and drive T cells in the primary HLH mouse model, we measured DC population in the TPM mice. There was an increase in the number of plasmacytoid DCs (pDCs) in the early stage but not in the number of conventional DCs (cDCs) (Figure 5A-C). However, at a later time, there was no significant difference in numbers of pDCs and cDCs between the TPM mice and the control mice (*Online Supplementary Figure S8*).

Macrophage activation by diverse triggers is a common feature in HLH. We found type 1 polarization of macrophages in both primary and sHLH models; thus, we investigated the macrophage population in TPM mice. The number of macrophages was significantly increased in the spleen, but not in the bone marrow in TPM mice (Figure 5D and G). More importantly, the macrophages were polarized toward type 1 in both bone marrow and spleen from the TPM mice (Figure 5E, F, H and I). To further determine whether type 1 polarized macrophages are able to phagocytose erythrocytes and cause anemia, we cultured erythroblasts with IFN- $\gamma$ -polarized type 1 bone marrow-derived macrophages (BMDMs) or IL-4-polarized type 2 BMDMs and found that only type 1 macrophages, but not type 2 macrophages, engulfed erythroblasts (Figure 5J-L and *Online Supplementary Figure S9*). Taken

together, our data suggest that HIF1A signaling activation causes type 1 macrophage polarization, which might also contribute to engulfment of erythroblasts and cause anemia in the HLH disease scenario.

#### Adaptive immune cells are not required for TPM-induced HLH phenotypes

Since there was no change in the frequency of the total and IFN- $\gamma$  producing CD8<sup>+</sup> T cells in the TPM mice, we further investigated the role of the lymphocytes in TPM-induced HLH phenotypes. We crossed *Vav1-Cre*/TPM mice with recombination activation gene 1 (*Rag1*)-deficient (*Rag1<sup>-/-</sup>*) mice that lack T cells and B cells (Figure 6A-B) and generated *Rag1<sup>-/-</sup>/Vav1-Cre*/TPM mice. *Rag1<sup>-/-</sup>/Vav1-Cre*/WT mice served as control. After administration of doxycycline, *Rag1<sup>-/-</sup>/Vav1-Cre*/TPM developed similar anemia, thrombocytopenia, and splenomegaly as the *Vav1-Cre*/TPM mice (Figure 6C and D). Type 1 macrophage polarization was also observed in *Rag1<sup>-/-</sup>/Vav1-Cre*/TPM mice (Figure 6E). Survival of *Rag1<sup>-/-</sup>/Vav1-Cre*/TPM mice was not prolonged compared to *Vav1-Cre*/TPM mice (Figure 6F). These data indicate that adaptive immunity is not essential for TPM-induced HLH phenotypes and non-lymphoid cells are sufficient to mediate disease progression in TPM mice.

#### Genetically blocking IFN- $\gamma$ signaling could not rescue TPM-induced phenotypes except to partly rescue the anemia

IFN- $\gamma$  is a critical factor upstream of HIF1A for type 1 macrophage polarization and is essential for disease development in the LCMV-infected *Prf1<sup>-/-</sup>* HLH mouse model. Thus, we determined the role of IFN- $\gamma$  signaling in TPM-induced HLH. We generated *Ifngr<sup>-/-</sup>/Vav1-Cre* /TPM (*Ifngr<sup>-/-</sup>/TPM*) mice. *Ifngr<sup>-/-</sup>/Vav1-Cre* /WT (*Ifngr<sup>-/-</sup>/WT*) mice served as control. Interestingly, TPM-induced anemia was partially rescued in *Ifngr* deficient mice (Figure 7A). However, the *Ifngr<sup>-/-</sup>/TPM* mice still developed severe thrombocytopenia (Figure 7B) and all of them succumbed to disease, but with a prolonged latency compared to the *Vav1-Cre*/TPM mice (Figure 7C). Flow cytometric analysis revealed that TPM-induced type 1 polarization of macrophages was not blocked in *Ifngr*-deficient mice (Figure 7D). We also generated *Ifngr<sup>-/-</sup>/Vav1-Cre* /TPM (*Ifngr<sup>-/-</sup>/TPM*) mice and found similar results (*Online Supplementary Figure S10*) indicating that HIF1A-induced HLH-like phenotypes in TPM mice are independent of IFN- $\gamma$  ligand and receptor. It is likely that IFN- $\gamma$  ligand and receptor are the upstream of HIF1A signaling, and HIF1A activation itself could lead to type 1 macrophage polarization to some degree even without IFN- $\gamma$  ligand and receptor. To determine whether IFN- $\gamma$  could induce HIF1A signaling and cause type 1 polarization in macrophages, we treated the mouse macrophage cell line, Raw264.7 cells, with IFN- $\gamma$ . We found that the level of HIF1A protein and the expression of known HIF1A target genes, including the critical macrophage polarization gene *Nos2*, are significantly increased in the IFN- $\gamma$  treated Raw264.7 cells compared to the control (Figure 7E and F). We also cultured BMDMs from TPM mice and induced TPM expression *in vitro*. We found an increase in mRNA expression of macrophage polarization-related gene (*Nos2*), glycolysis-related genes (*Hlk2*, *Pfklb3*), and also other HIF1A direct target genes (*Adm*) (Figure 7G and H). These genes were similarly activated by IFN- $\gamma$  when treated with Raw264.7

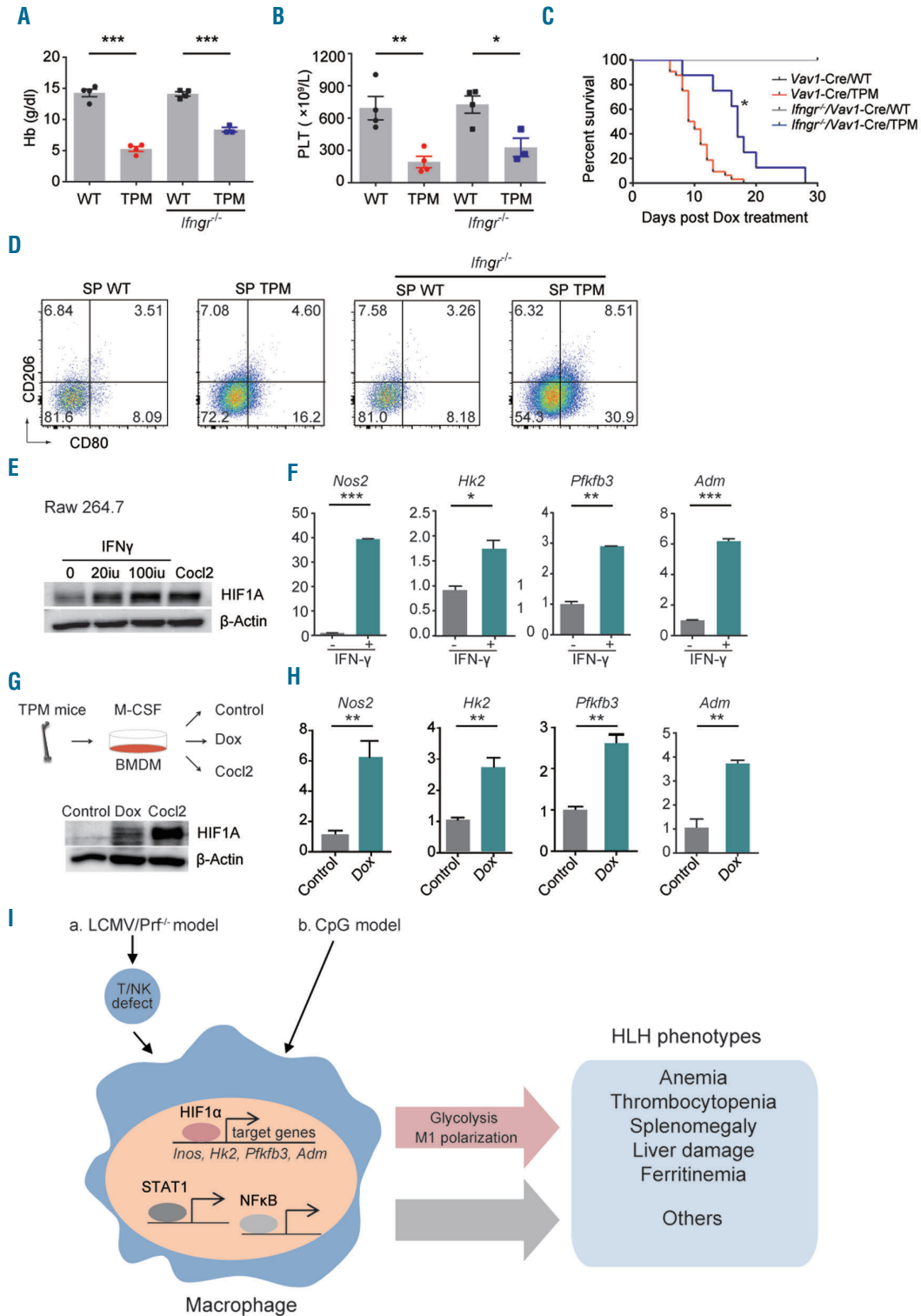


**Figure 7. Genetic deletion of IFN- $\gamma$  receptor cannot rescue the triple point mutation (TPM) induced hemophagocytic lymphohistiocytosis (HLH)-like phenotypes.** (A-D) *Ifngr*<sup>-/-</sup>/Vav1-Cre/LSL/TPM (*Ifngr*<sup>-/-</sup>/TPM) mice were generated. *Ifngr*<sup>-/-</sup>/Vav1-Cre/LSL/WT [*Ifngr*<sup>-/-</sup>/wild-type (WT)] mice served as their control. *Ifngr*<sup>-/-</sup>/TPM, *Ifngr*<sup>-/-</sup>/WT, Vav1-Cre/TPM, Vav1-Cre/WT mice were administered with doxycycline. (A and B) Hemoglobin (Hb) (A) and platelets (PLT) (B) on day (d)8 after doxycycline induction. (C) Kaplan-Meier analysis of survival of *Ifngr*<sup>-/-</sup>/TPM (n=8), *Ifngr*<sup>-/-</sup>/WT (n=8), Vav1-Cre/TPM (n=32), Vav1-Cre/WT (n=26) mice. Statistical analysis showed that there was a significant difference between *Ifngr*<sup>-/-</sup>/TPM and *Ifngr*<sup>-/-</sup>/WT mice ( $P < 0.0001$ ), and between *Ifngr*<sup>-/-</sup>/TPM and Vav1-Cre/TPM mice ( $P < 0.05$ ). (D) Representative flow cytometry CD80/CD206 scatter dot plots of splenic macrophages in the indicated mice. (E) Cell lysates of IFN- $\gamma$  (20 IU/mL or 100 IU/mL as final concentration) or Coc12-treated Raw264.7 cells were analyzed for HIF1A and  $\beta$ -Actin by western blot. (F) Raw264.7 cells were treated with or without IFN- $\gamma$  (100 IU/mL as final concentration) for 24 hours (h). mRNA expression of the indicated genes was shown by qRT-PCR. (G) Schematic diagram showing Vav1-Cre/TPM mice-derived BMDM turning on expression of HIF1A/ARNT following addition of doxycycline *in vitro* (top). HIF1A protein level in doxycycline-treated or untreated Vav1-Cre/TPM mice-derived BMDM measured by western blot (bottom). (H) Relative mRNA expression of the indicated genes was shown by qRT-PCR. (I) Working model for the role of HIF1A in HLH. \* $P < 0.05$ , \*\* $P < 0.01$ , \*\*\* $P < 0.001$  versus control for all experiments.

cells (Figure 7F). The evidence suggests that HIF1A signaling is the downstream of IFN- $\gamma$  signaling and that activation of HIF1A signaling could activate and polarize macrophages which results in some key features of HLH-like phenotypes. Activation of HIF1A signaling in combination with activation of other pathways, such as NF- $\kappa$ B and STAT1, might lead to the complete complex HLH phenotypes as seen in humans (Figure 7I).

## Discussion

Although there are differences in etiology and pathological immune response between FHL patients and sHLH patients, they have similar clinical manifestations and the same features of hyper-inflammation and hyper-immune response.<sup>27</sup> Identification of key common mediators in HLH may help to explore novel therapeutic targets that would have a wider application in HLH patients. In the present study, we identified that the HIF1A signature is enriched in both FHL and sJIA patients, and its protein level is elevated in primary and sHLH mouse models. Induction of HIF1A signaling in hematopoietic cells *in vivo* results in HLH-like phenotypes. This indicates that HIF1A is a critical mediator for HLH.

HIF1A is reported to be involved in inflammation and immune response.<sup>10,12,32</sup> In line with this, our bioinformatic analysis of FHL and sJIA datasets revealed that HIF1A might have a wide regulatory effect in HLH pathogenesis, which may be related to regulation of chemotaxis, cytokines, immune response, glycolysis, blood coagulation, and apoptosis, as indicated by the GO analysis. Notably, it is evident that FHL patients have a stronger signature than sJIA patients. This could be due to the independent processes of these two array datasets from both groups. There is also a possibility that the strong genetic component of FHL leads to this discrepancy. However, we did not observe a significant difference in the HIF1A signature between FHL patients with and those without a genetic diagnosis in this dataset. It is hard to completely rule out the possibility that genetic mutation drives HIF1A signature since only mutations of *PRF1*, *UNC13D*, and *STX11* were tested in this FHL microarray dataset.<sup>21</sup> Patients without a genetic diagnosis may still carry disease-causing mutations. Future studies are needed to clarify whether the strong genetic background could have additional effects on the gene signatures. Nonetheless, the stronger signature in FHL patients as compared to the sJIA patients could be the underlying difference between these two diseases, and it is possible that the involvement of distinct cell types causes this difference. T cells, NK cells, macrophages, and DCs are all involved in the FHL pathogenesis, while T cells and NK cells are less involved in the sJIA pathogenesis.<sup>33</sup> Thus, in microarray datasets of PBMCs, FHL may show a stronger signature than sJIA.

Macrophage activation/polarization is a common feature in HLH mouse models irrespective of their specific etiology. Macrophages have been reported to switch their metabolism from oxidative phosphorylation towards glycolysis upon pro-inflammatory stimuli by the upregulation of HIF1A.<sup>34,35</sup> Indeed, we found that HIF1A was stabilized in macrophages in both the LCMV/*Prf1*<sup>-/-</sup> model and the CpG model. Our data are consistent with other reports that numerous stimuli, such as IFN- $\gamma$ , TNF- $\alpha$ , CpG, and LPS, are able to increase the HIF1A protein level

in macrophages.<sup>10</sup> These cytokines and TLR ligation might co-operate to increase HIF1A protein levels in HLH.

Although several studies have showed an HIF1A deficiency in myeloid cells leads to impaired inflammatory responses, the effect of activation of HIF1A in hematopoietic cells *in vivo* remains unclear. Here, we show that induction of HIF1A in hematopoietic cells *in vivo* is lethal and gives rise to some HLH-like phenotypes, such as severe anemia, thrombocytopenia, splenomegaly, liver damage, ferritinemia, and macrophage activation, suggesting that HIF1A is a critical mediator in HLH. We are also aware that HIF1A-induced phenotypes cannot recapitulate all the manifestations seen in human HLH patients. This could be due to the fact that other transcription factors which co-operate with HIF1A activation to generate the overt HLH phenotypes are required. Our analysis of the transcription factor network sheds light on other key transcription factors in HLH development which could help in future research.

Defective CD8<sup>+</sup> T cells are regarded as the driver in the primary HLH mouse model.<sup>5</sup> However, the HLH-like phenotypes in the TPM mouse model are not dependent on lymphocytes since activation of HIF1A also causes HLH phenotypes in *Rag1*<sup>-/-</sup> mice. This indicates that non-lymphocytes contribute to the HLH-like phenotypes. Here, we observed that HIF1A activation leads to macrophage type 1 polarization *in vivo*. Our *in vitro* data and other reports revealed that HIF1A can up-regulate *Nos2*, *IL-6*, *IL-1 $\beta$* , *CXCR4* and, glycolysis-related genes which might account for the *in vivo* type 1 polarization.<sup>32</sup> The role of type 1 polarization of macrophages for anemia in HLH is still unclear. Our *in vitro* data show that IFN- $\gamma$ -polarized type 1 macrophages engulf erythroblasts, which is consistent with our earlier report<sup>36</sup> that IFN- $\gamma$  acts directly on macrophages resulting in hemophagocytosis, leading to a consumptive anemia *in vivo*. There is also evidence that hemophagocytes express type 2 polarized macrophage markers such as CD206 or CD163, and exhibit expression profiles similar to resting splenic macrophages.<sup>37,38</sup> This discrepancy in distinct macrophage activation type may be due to a different subpopulation of macrophage, or to various different etiological scenarios. Although IFN- $\gamma$ -polarized type 1 macrophages phagocytose erythroblasts in our *in vitro* experiment setting, robust phagocytosis was not observed in the TPM mice, which suggests that type 1 polarization of macrophages induced by HIF1A transgene is not sufficient to induce hemophagocytosis *in vivo*.<sup>24,39,40</sup> Other additional factors, such as blocking IL-10 signaling or involvement of DCs may be required for phagocytosis *in vivo*. Future investigation will be needed to verify these possibilities.

IFN- $\gamma$  is a potent stimulator for type 1 macrophage polarization, and plays a central role in a large proportion of HLH patients and in FHL mouse models; however, it has also been seen that it is not essential in some of the sHLH mouse models.<sup>39,41</sup> Our study also showed that TPM-induced HLH-like phenotypes are independent of IFN- $\gamma$ . In fact, our *in vitro* data and other reports showed that HIF1A is a downstream effector of IFN- $\gamma$ , and activation of HIF1A in macrophages leads to the increase in type 1 polarization-related genes, such as *Nos2*, and other glycolysis-related genes. However, partial rescue of anemia was observed in TPM mice with IFN- $\gamma$  deficiency. IFN- $\gamma$  may also have HIF1A-independent mechanisms that affect erythropoiesis, as has been reported.<sup>42</sup>

In summary, our study suggests that HIF1A is a common critical downstream mediator for HLH. We propose that HIF1A activation as the consequence of systemic inflammation, cytokine storm, or ligation of TLR may contribute to HLH development. Thus, HIF1A might be a promising therapeutic target for HLH intervention.

### Acknowledgments

The authors would like to thank Eric VIVIER who kindly provided the transgenic mice.

### Funding

This work was supported by a Pilot Grant of The HLH Center of Excellence at Cincinnati Children's Hospital Medical Center

(to GH), and a grant from Histiocytosis Association Research Grant Program (to GH), Southern Medical University Basic Research Grant Program (No. QD2016N016 to RH), Natural Science Foundation of Guangdong Province, China (No. 2017A030310112 to RH), National Natural Science Funds of China (No. 81300392 to JW, No.81370611 to ZFX, No. 81470338 to YZ, No. 81470297, and No. 81770129, to GH, and No. 81530008, and No. 81470295 to ZJX, No. 81570173 to XL), Tianjin science and technology projects (13JCYBJC42400 to YZ). We would like to acknowledge the assistance of the Research Flow Cytometry Core in the Division of Rheumatology at Cincinnati Children's Hospital Medical Center. All flow cytometric data were acquired using equipment maintained by the Research Flow Cytometry Core.

## References

- Janka GE, Lehmborg K. Hemophagocytic lymphohistiocytosis: pathogenesis and treatment. *Hematology Am Soc Hematol Educ Program*. 2013;2013:605-611.
- Jordan MB, Allen CE, Weitzman S, Filipovich AH, McClain KL. How I treat hemophagocytic lymphohistiocytosis. *Blood*. 2011;118(15):4041-4052.
- Lehmborg K, Nichols KE, Henter JJ, et al. Consensus recommendations for the diagnosis and management of hemophagocytic lymphohistiocytosis associated with malignancies. *Haematologica*. 2015;100(8):997-1004.
- Filipovich AH, Chandrakasan S. Pathogenesis of Hemophagocytic Lymphohistiocytosis. *Hematol Oncol Clin North Am*. 2015;29(5):895-902.
- Jordan MB, Hildeman D, Kappler J, Marrack P. An animal model of hemophagocytic lymphohistiocytosis (HLH): CD8+ T cells and interferon gamma are essential for the disorder. *Blood*. 2004;104(3):735-743.
- Lehmborg K, Sprekels B, Nichols KE, et al. Malignancy-associated haemophagocytic lymphohistiocytosis in children and adolescents. *Br J Haematol*. 2015;170(4):539-549.
- Brisse E, Wouters CH, Matthys P. Advances in the pathogenesis of primary and secondary haemophagocytic lymphohistiocytosis: differences and similarities. *Br J Haematol*. 2016;174(2):203-217.
- Emile JF, Ablu O, Fraitag S, et al. Revised classification of histiocytoses and neoplasms of the macrophage-dendritic cell lineages. *Blood*. 2016;127(22):2672-2681.
- Fall N, Barnes M, Thornton S, et al. Gene expression profiling of peripheral blood from patients with untreated new-onset systemic juvenile idiopathic arthritis reveals molecular heterogeneity that may predict macrophage activation syndrome. *Arthritis Rheum*. 2007;56(11):3793-3804.
- Palazon A, Goldrath AW, Nizet V, Johnson RS. HIF transcription factors, inflammation, and immunity. *Immunity*. 2014;41(4):518-528.
- Greer SN, Metcalf JL, Wang Y, Ohh M. The updated biology of hypoxia-inducible factor. *EMBO J*. 2012;31(11):2448-2460.
- Cummins EP, Keogh CE, Crean D, Taylor CT. The role of HIF in immunity and inflammation. *Mol Aspects Med*. 2016;47-48:24-34.
- Cramer T, Yamanishi Y, Clausen BE, et al. HIF-1alpha is essential for myeloid cell-mediated inflammation. *Cell*. 2003;112(5):645-657.
- Walmsley SR, Chilvers ER, Thompson AA, et al. Prolyl hydroxylase 3 (PHD3) is essential for hypoxic regulation of neutrophilic inflammation in humans and mice. *J Clin Invest*. 2011;121(3):1053-1063.
- Jantsch J, Chakravorty D, Turza N, et al. Hypoxia and hypoxia-inducible factor-1 alpha modulate lipopolysaccharide-induced dendritic cell activation and function. *J Immunol*. 2008;180(7):4697-4705.
- McNamee EN, Korns Johnson D, Homann D, Clambey ET. Hypoxia and hypoxia-inducible factors as regulators of T cell development, differentiation, and function. *Immunol Res*. 2013;55(1-3):58-70.
- Imtiyaz HZ, Williams EP, Hickey MM, et al. Hypoxia-inducible factor 2alpha regulates macrophage function in mouse models of acute and tumor inflammation. *J Clin Invest*. 2010;120(8):2699-2714.
- Doedens AL, Phan AT, Stradner MH, et al. Hypoxia-inducible factors enhance the effector responses of CD8(+) T cells to persistent antigen. *Nat Immunol*. 2013;14(11):1173-1182.
- Blouin CC, Page EL, Soucy GM, Richard DE. Hypoxic gene activation by lipopolysaccharide in macrophages: implication of hypoxia-inducible factor 1alpha. *Blood*. 2004;103(3):1124-1130.
- Albina JE, Mastrofrancesco B, Vessella JA, Louis CA, Henry WL Jr, Reichner JS. HIF-1 expression in healing wounds: HIF-1alpha induction in primary inflammatory cells by TNF-alpha. *Am J Physiol Cell Physiol*. 2001;281(6):C1971-1977.
- Sumegi J, Barnes MG, Nestheide SV, et al. Gene expression profiling of peripheral blood mononuclear cells from children with active hemophagocytic lymphohistiocytosis. *Blood*. 2011;117(15):e151-160.
- Bridges JP, Lin S, Ikegami M, Shannon JM. Conditional hypoxia inducible factor-1alpha induction in embryonic pulmonary epithelium impairs maturation and augments lymphangiogenesis. *Dev Biol*. 2012;362(1):24-41.
- Narni-Mancinelli E, Chaix J, Fenis A, et al. Fate mapping analysis of lymphoid cells expressing the Nkp46 cell surface receptor. *Proc Natl Acad Sci USA*. 2011;108(45):18324-18329.
- Behrens EM, Canna SW, Slade K, et al. Repeated TLR9 stimulation results in macrophage activation syndrome-like disease in mice. *J Clin Invest*. 2011;121(6):2264-2277.
- Das R, Guan P, Sprague L, et al. Janus kinase inhibition lessens inflammation and ameliorates disease in murine models of hemophagocytic lymphohistiocytosis. *Blood*. 2016;127(13):1666-1675.
- Grom AA, Villanueva J, Lee S, Goldmuntz EA, Passo MH, Filipovich A. Natural killer cell dysfunction in patients with systemic-onset juvenile rheumatoid arthritis and macrophage activation syndrome. *J Pediatr*. 2003;142(3):292-296.
- Ravelli A, Grom AA, Behrens EM, Cron RQ. Macrophage activation syndrome as part of systemic juvenile idiopathic arthritis: diagnosis, genetics, pathophysiology and treatment. *Genes Immun*. 2012;13(4):289-298.
- Villanueva J, Lee S, Giannini EH, et al. Natural killer cell dysfunction is a distinguishing feature of systemic onset juvenile rheumatoid arthritis and macrophage activation syndrome. *Arthritis Res Ther*. 2005;7(1):R30-37.
- Emig D, Salomonis N, Baumbach J, Lengauer T, Conklin BR, Albrecht M. AltAnalyze and DomainGraph: analyzing and visualizing exon expression data. *Nucleic Acids Res*. 2010;38(Web Server issue):W755-762.
- Chow A, Lucas D, Hidalgo A, et al. Bone marrow CD169+ macrophages promote the retention of hematopoietic stem and progenitor cells in the mesenchymal stem cell niche. *J Exp Med*. 2011;208(2):261-271.
- Balsamo M, Manzini C, Pietra G, et al. Hypoxia downregulates the expression of activating receptors involved in NK-cell-mediated target cell killing without affecting ADCC. *Eur J Immunol*. 2013;43(10):2756-2764.
- Lin N, Simon MC. Hypoxia-inducible factors: key regulators of myeloid cells during inflammation. *J Clin Invest*. 2016;126(10):3661-3671.
- Mellins ED, Macaubas C, Grom AA. Pathogenesis of systemic juvenile idiopathic arthritis: some answers, more questions.

- Nat Rev Rheumatol. 2011;7(7):416-426.
34. Gordan JD, Thompson CB, Simon MC. HIF and c-Myc: sibling rivals for control of cancer cell metabolism and proliferation. *Cancer Cell*. 2007;12(2):108-113.
  35. Liu L, Lu Y, Martinez J, et al. Proinflammatory signal suppresses proliferation and shifts macrophage metabolism from Myc-dependent to HIF1alpha-dependent. *Proc Natl Acad Sci USA*. 2016; 113(6):1564-1569.
  36. Zoller EE, Lykens JE, Terrell CE, et al. Hemophagocytosis causes a consumptive anemia of inflammation. *J Exp Med*. 2011; 208(6):1203-1214.
  37. Canna SW, Costa-Reis P, Bernal WE, et al. Brief report: alternative activation of laser-captured murine hemophagocytes. *Arthritis Rheum*. 2014;66(6):1666-1671.
  38. McCoy MW, Moreland SM, Detweiler CS. Hemophagocytic macrophages in murine typhoid fever have an anti-inflammatory phenotype. *Infect Immun*. 2012; 80(10):3642-3649.
  39. Canna SW, Wrobel J, Chu N, Kreiger PA, Paessler M, Behrens EM. Interferon-gamma mediates anemia but is dispensable for fulminant toll-like receptor 9-induced macrophage activation syndrome and hemophagocytosis in mice. *Arthritis Rheum*. 2013;65(7):1764-1775.
  40. Ohyagi H, Onai N, Sato T, et al. Monocyte-derived dendritic cells perform hemophagocytosis to fine-tune excessive immune responses. *Immunity*. 2013; 39(3):584-598.
  41. Avau A, Mitera T, Put S, et al. Systemic juvenile idiopathic arthritis-like syndrome in mice following stimulation of the immune system with Freund's complete adjuvant: regulation by interferon-gamma. *Arthritis Rheumatol*. 2014;66(5):1340-1351.
  42. Lin FC, Karwan M, Saleh B, et al. IFN-gamma causes aplastic anemia by altering hematopoietic stem/progenitor cell composition and disrupting lineage differentiation. *Blood*. 2014;124(25):3699-3708.